Helicopter Flap/Lag Energy Exchange Study

S. Castillo-Rivera and M. Tomas-Rodriguez

School of Mathematics, Computer Science & Engineering.
City University of London. United Kingdom

(Corresponding author, email: Salvador.Castillo-Rivera.1@city.ac.uk)

January 22, 2017

Abstract

This paper presents a study on the energy exchange taking place on articulated helicopter main rotor blades. The blades are hinged and the flap/lag modes are highly coupled. These dynamical couplings existing between the two degrees of freedom are clearly identifiable as the nonlinear terms that appear in the equations of motion, are key to understand the energy exchange process. The work here conducted is carried out using VehicleSim, a multibody software specialized in modelling mechanical systems composed by rigid bodies. A spring pendulum system is also studied in order to examine its nonlinear behaviour, and to establish existing analogies with the rotor blade nonlinear dynamics. The nonlinear couplings of both systems are compared to each other, and commensurability condition is analysed by means of Short Time Fourier Transform (STFT) methods as well as the flap and lag amplitudes spectrum. Simulations are carried out and the obtained results show clear analogies in the energy exchange process taking place in both systems. The stability of these modes is also studied using Poincare' map method.

Keywords: Flap, Lag, Nonlinear, Commensurability, Energy

1 Introduction

Helicopters are highly nonlinear systems, inherently unstable by nature and they are mechanically complex composed of various bodies with several degrees of freedom and exhibit general motions in all three dimensions. Helicopter's vibration has been a problem from the earliest days of helicopter development and it has a direct impact on the production as well as the maintenance costs. Vibrations, in general, constitute a hostile environment for all kinds of equipment [1].

In helicopter studies, experimental data related to several flight conditions are significantly limited due to practical and economical reasons. This difficulty can be overcome by using simulations in order to evaluate the applicability of

a model identification scheme and to validate the test of systems for the helicopter. The main goal in this work is to understand the energy exchange that takes place between the flap and lag modes of a main rotor blade that may be behind vibrations appearing on the rotor.

Since the 1990's, several multibody dynamics softwares have been implemented and developed in the rotorcraft field. Multibody dynamics approach is useful in order to deal with complex mechanisms with great variety of shapes such as the mechanisms found in rotors. On the other hand, small perturbations theory is very often applied to the equations to simplify their analytical solution. However, for more advanced applications, a fully descriptive nonlinear form of the equations should be obtained if couplings and energy exchange processes need to be studied. These equations are difficult to solve analytically. VehicleSim provides the nonlinear dynamic equations in three dimensions, this is a novel feature with respect to previous work presented in Chen [2], where the author did a complete work on the flap/lag nonlinear dynamical equations of motion. Three hinges sequences were used in order to obtain the equations of the lag-feather-flap, flap-feather-lag, flap-lag-feather motions. In this case, the Lagrange method was used to derive the coupled equations of motion.

Main rotor blade dynamics contain general nonlinear terms in their equations, real blades can be expected to show behavioural properties of general nonlinear dynamical systems [3]. Such behaviour will be associated to larger amplitudes of vibration, where the nonlinear terms increase in relative relevance. It is also implied that they will be associated to unusual operating circumstances. Understanding the nonlinear behaviour of main rotor blades is relevant as these have implications on helicopter design, pilot training, flight condition and accident investigation.

Procedures for identifying particular terms on the nonlinear equations of motion should be proposed and the corresponding operating conditions should be identified in order to understand nonlinear behaviour, particularly in the case of main rotor blades with two degrees of freedom (flap and lag) as they are highly coupled.

An autoparametric system can be established as a nonlinear dynamic system in which the time variation of a system's parameter in the primary system is not clear, on the contrary, it is dependent on the motion of the second system by means of nonlinear terms. Saved et al. [4] studied the response to harmonic excitations for a two degrees of freedom, autoparametric system and controlled. The authors analysed the impact of a linear absorber on the vibrating system as well as the saturation control of a linear absorber to diminish vibrations because of rotor blade flap displacement. The method of multiple scale perturbation technique was used to derive the periodic response equation close to the primary resonance in the presence of internal resonance of the system. An active vibration absorber to remove the high amplitude vibration of the nonlinear plant was studied in the presence of 1:1 internal resonance, being the plant under the influence of primary external excitation. Saturation phenomenon, internal resonance used to control the steady state as well as transient vibrations of a plant were studied by using perturbation analysis and numerical simulation. The re-

sults showed that saturation control of steady state vibrations was efficient, and in good agreement with the theory. The authors extended these results in Saved et al. [5] where an active vibration absorber to eliminate the vibration of a nonlinear system was analysed in the presence of 1:2 and 1:3 internal resonance. In addition, the plant was subjected to external and parametric excitations. The work focused on the study of an active control and stability characterics of two systems which were employed to diminish vibrations because of rotor blade flap dynamics. The method of multiple scale perturbation technique was used to calculate four first order nonlinear ordinary differential equations in the presence of internal resonance of the two systems with quadratic and cubic control order. These equations were applied to find the steady state solutions and their stability. The stability of the obtained numerical solution was also studied using both phase plane methods and frequency response equations. The results were compared to previous results and shown to agree with the corresponding references.

In Santos et al. [6] the authors carried out a theoretical and experimental contribution to the problem of rotor blades' dynamic interaction. The blades were shaped as Euler-Bernoulli beams. Three approaches to define the beam deformation were provided: i) linear model ii) linear beam model with second order terms and iii) a complete nonlinear model. The mathematical models validation used a simple test rig, built by a mass-spring system connected to four flexible rotating blades. The linear model could calculate parametric vibrations for a short range of low rotational speed, wherein the stiffening impact is of minor magnitude. Superharmonic vibration associated to the dynamics of the flexible rotating parts could be identified by using the full nonlinear model. On the other hand, in Tekin et al. [7], the nonlinear vibrations of multiple Euler-Bernoulli stepped beams were analysed. A 3:1 internal resonance case was studied for the system. A general approach to obtain a solution to the problem was derived using the method of multiple scales. The equations of motions were derived by Hamilton's principle and made dimensionless. The method of multiple scales was applied to calculate the general modulation equations of the amplitude and phases for two interacting modes. The force-response, damping-response and frequency-response curves were plotted for the internal resonance modes of vibrations and finally, a stability study was done.

Nonlinear damping suspension and its effect on a flexible rotor in journal bearings has been studied in Yan et al. [8]. A computational method was applied to derive the equations of motion. The results showed that the rotor speed determines the effect of the nonlinear damping suspension on the motions of the system. In fact, for low speeds, the plant presented the same displacement as the pattern under the nonlinear damping suspension. However for high speeds, the impact of nonlinear damping is determined by a combination of the damping exponent and damping coefficient.

The study of coupled motions in dynamical systems is relevant, as it allows to identify mechanisms of transference of energy between different modes of oscillation. This energy exchange has been studied before i.e., in the case of a ship. Nayfeh et al. [9] formulated and analysed quadratic roll/pitch equations of motions and parametric excitations subject to a 2:1 internal resonance

condition where the pitch natural frequency was the double of the roll mode in regular sea conditions. The authors observed that the amplitude of the roll mode was larger than the pitch mode, for large excitations amplitudes. Under severe weather conditions, the equations of motions needed to take into account the nonlinearities of the large amplitude ship motion. As a consequence of this, Ibrahim et al. [10] showed the coupled nonlinear equations of motion in heave, roll, and pitch based on physical grounds. An overview of the roll dynamic stability under random sea waves was presented in terms of the sample stability conditions and response statistical moments. In addition to this work, an apparently completely different system such as a motorcycle, has revealed the presence of burst of steering oscillations under high speed acceleration conditions, see Simos et al. [11]. Once the oscillations began, they persisted with a frequency of the order of 28 rad/s, which was consistent with weave-type behaviour. Furthermore, the transfer of energy and control of the vibrations on microelectromechanical system gyroscope with linear and nonlinear parametric excitations was investigated in Hamed et al. [12]. The problem was defined by two degrees of freedom system of nonlinear ordinary differential equations. The coupling of the plant equations was due to energy transfers between the two vibration modes and the resonance in the system.

Recent studies have confirmed that any vector field is able to decompose in rotational field and gradient via Helmholtz's theorem. The transmission of energy takes place for the propagation of electromagnetic wave matching with the variation of electromagnetic field, thereby the dynamical oscillators and neurons are able to absorb and release energy in presence of electromagnetic conditions. In fact, Chun-Ni et al. [13] have analysed the estimation of Hamilton energy for a class of dimensionless dynamical systems using Helmholtz's theorem. The nonlinear oscillating circuits can be drawn up into dynamical systems through scale transformation; this can be used to work out dynamical equations for the realistic nonlinear oscillating circuit. In this way, the Hamilton energy function could be derived effectively and this is useful for self-adaptively controlling dynamical systems.

Xin-Lin et al. [14] have studied the energy shift induced by transition of electric modes in a Hindmarsh-Rose neuron by using the Helmholtz's theorem. It was figured out that the energy storage was dependent on the external forcing and the energy release was associated with the electric mode. A nonlinear circuit was set up using resistor, capacitor and inductor among others electric components. In addition, the electromagnetic field energy was released from the circuit in the oscillating state. As a consequence of this, the chaotic and bursting states were useful to release the energy in the neuron swiftly. It is known that the controllers created as piecewise-linear are employed to produce multi-scroll attractors in nonlinear circuits creating a group of equilibrium points. Li et al. [15] presented a practical outline which was able to produce infinite-scroll attractor by changing the nonlinear terms in the Chua circuit with a sine function. The Hamilton energy of the circuit integrated of multi-scroll attractor was reduced with the rising number of multi-scroll attractor. Showing this result that power consumption of circuit devices could be reduced when multi-scroll attractor was stabilized. In this work, the Hamilton energy of the circuit was determined by the Helmholtz's theorem.

Sarasola et al. [16] presented a method to assign to a chaotic system of known dynamics a function of the phase space variables with the characteristics of energy. It was studied and discussed the flows of energy at different values of the coupling strength for nonidentical synchronization between Chua guided, Rssler and Lorenz systems. The contribution to the dissipated energy was able to work out in terms of two components: a) the component related with the trajectory described in phase space by the stable steady states caused by the coupling in the guided system. b) The rest of the dispersed energy was able to be in some way associated to the accomplishment of the synchronization in phase and frequency. The energy dissipated by the system appeared to be sensitive to the transitions in the stability of their equilibrium points caused by the coupling.

Nowadays the synchronization study is focused on physical, mechanical systems among others. Hou et al. [17] have studied two co-rotating rotors fast excited by induction motors installed in a vibrating body. The stability criterion and synchronization condition of the system were figured out using the energy balance method. The stable phase difference and synchronization zones were calculated by the two co-rotating rotors operated in synchronous state. It was confirmed that the dynamic characteristics of the vibrating body were linked to the synchronous state of the system.

Zhou et al. [18] analysed the influence of the external and load excitations, the internal system parameters as well as the equilibrium positions on the dynamic responses of nonlinear tristable energy harvesters using the harmonic balance method. Numerical simulations and experimental results were carried out to support the theoretical analysis. The theoretical results showed that the external electrical load presented a low influence on the corresponding dynamic response. The voltage and the displacement responses diminished their magnitudes with the system damping. Theoretical and numerical results displayed that the tristable energy harvester with a shorter distance between the equilibrium positions presented smaller excitation amplitude and larger number of initial conditions to realize high energy interwell oscillations.

The objective of this article is to study the nonlinear behaviour and energy exchange that characterizes a helicopter rotor blade with flap and lag degrees of freedom. The nonlinear dynamical equations of the system -obtained via VehicleSim- will be analysed by studying an equivalent spring pendulum system that has two coupled degrees of freedom whose dynamical characteristics can resemble those of the coupled flap/lag motions. The aim therefore is to identify particular terms in the nonlinear equations of motion that can shed on light energy exchange being this something that should be considered as proposed by Saved et al. [5] and Tekin et al. [7]. The nonlinear equations obtained represent an advantage with respect to the work presented in Chen [2] and Tekin et al. [7], as it finds analogies with nonlinear systems, allowing to predict some behaviour on the system under study. This is an advantage with respect to Santos et al. [6] and Tekin et al. [7]. In addition, in order to test the impact of the rotor angular speed and the damping coefficient on the blade, the results proposed by Yan et al. [8] are considered. Furthermore, this article presents a system with two degrees of freedom coupled where the transference of energy

is studied, being it an additional contribution in the line of the work presented by [9–12].

VehicleSim provides the nonlinear equations of motions in three dimensions, these equations are obtained as a consequence of a modelling process. Once the exchange of energy will be tested for the coupled flap/lag motion, this system should be analysed according to the studies presented by [13,16–18]. Therefore, a theoretical approach of the problem should be carried out, in order to obtain the Hamilton energy and the results reported by the references [13–15] should be taken into account. As a consequence of this, the oscillating energy could be compared with the Hamilton energy. According to Sarasola et al. [16] the energy function can be figured out in a generalized form as:

$$\dot{x} = M(x)\nabla H \tag{1}$$

where $M(x)$ is the local structure matrix and ∇H is the gradient vector of a smooth energy function $H(x)$. This could be carried out, however, it is not tackled due to the obtention of these functions should be calculated further of the VehicleSim features and this is out of the proposed goal for this article. In fact, it is a complex task primarily if the problem is dealt with in the three spatial dimensions. It should be properly presented in a future work.

In the view of these considerations, the main contributions of this paper can be summarized as follows: a) To present the nonlinear equations for a main rotor blade with flap and lag degrees of freedom derived in VehicleSim. b) To describe and discuss the mathematical behaviour of a spring pendulum as a nonlinear physical system. c) To identify mathematically equivalent nonlinear terms between spring pendulum and the main rotor blade equations, which provide implicit information about the complex coupled dynamic between the flap and the lag degrees of freedom. These analogies and the predictions figured out, provide an educational role to this article. Due to this serves to encourage further studies that help to describe the relationship between two systems seemingly not related. However, the study of their corresponding nonlinear equations of motions can show that their behaviours are not so unconnected. d) To present simulation results obtained with the main rotor blade nonlinear model, and to compare these to predicted behaviour.

The outline of the paper is as follows;
Section 2 describes the blade's mechanical structure and degrees of freedom, as well as VehicleSim main features and computing characteristics. Section 3 studies the spring pendulum nonlinear dynamics. Section 4 analyses the blade's flap/lag motions, and studies the transference of energy between these modes of oscillation. Finally, Section 5 summarizes the main conclusions.

2 Modelling

The main aim of this section is to describe the modelling developed for implementing the blade model. The general considerations of this are described in

the following lines.

2.1 Hinge and Blade Dynamics

The role of the main rotor is to support the rotorcraft's weight, as it generates the lift force. It allows to keep the helicopter suspended in the air and provides the control that allows to follow a prescribed trajectory by changing altitude and executing turns. It transfers prevailing aerodynamic forces and moments from the rotating blades to the non rotating frame (fuselage). The blades are kept in uniform rotational motion (rotational speed Ω) by a shaft torque from the engine. A common design solution adopted in the development of the helicopter is to use hinges at the blades roots that allow free motion of the blade normal to and in the plane of the disc (see Figure 1). The most common of these hinges is the flap hinge that allows the blade to flap, this is, to move in a plane containing the blade and the shaft, of the disc plane, about either the actual flap hinge or in some other cases, the flap hinge is substituted by a region of structural flexibility at the root of the blade. The flap hinge is more frequently designed to be at a short distance from the centre line. This is termed an "offset" (eR) and it offers the designer a number of important advantages [19, 20].

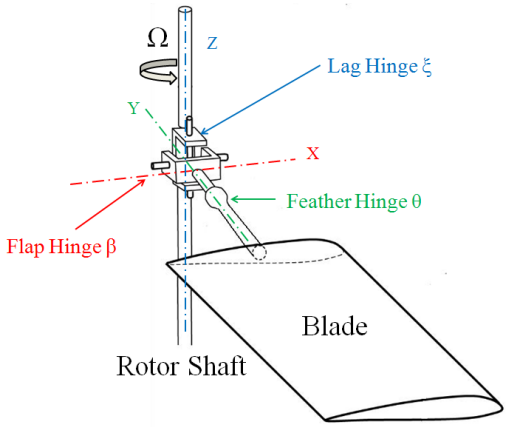

Figure 1: Schematic diagram of main rotor's hub and hinges system.

A blade that is free to flap, experiences large Coriolis moments in the plane of rotation and a further hinge, this is the lag hinge, is provided to relieve these moments. This degree of freedom allows the blade motion to be parallel to the disc plane [21, 22].

A blade can also feather around an axis parallel to the blade span. Blade feather motions are necessary to control the aerodynamic lift developed and, in forward motion of the helicopter, to allow the advancing blade to reach a lower angle of incidence than the retreating blade and thereby to balance the lift across the craft. In order for the helicopter to climb up, the feather angle needs to be increased. On the other hand, in order to descend, the blade's

feather angle is decreased. Because all blades are acting simultaneously in this case, this is known as collective feather and allows the rotorcraft to rise/fall vertically. Additionally to this control, in order to achieve forward, backward and sideways flight, a different additional change of feather is required. The feather on each individual blade is increased at the same selected point on its circular pathway. This is known as cyclic feather or cyclic control. Blade feather control is performed through a linkage of the blade to a swashplate [23, 24].

For VehicleSim modelling purposes, the following considerations are made regarding the physical structure of the main rotor (see [25, 26]):

- The main rotor consists of four equally spaced blades joined to a central hub. The blades have free motion in and out of the plane of the disc; this is allowed by the inclusion of flap and lag hinges.
- The blades are rigid.
- The rotor's angular speed is constant.

2.2 VehicleSim as Modelling Tool

Over the years, great efforts have been devoted to develop the helicopter simulation field. Nowadays, several computer packages for assisted mechanical modelling are available. VehicleSim Lisp is a computer program that allows to model, simulate as well as to derive symbolic equations of motion for mechanical systems composed of multiple rigid bodies. The VehicleSim code is used to generate a C simulation program, capable of computing general motions corresponding to specified cases with initial conditions and external forcing inputs.

VehicleSim solvers on Windows are compiled as dynamically linked library (DLL) files with a standard VehicleSim application program interface (API) that works with several possible simulation environments, including the VehicleSim browser and Matlab. The source code generated by VehicleSim Lisp is accessible by the user.

VehicleSim Lisp generates the equations of motion for a multibody system in symbolic form. Then a C source code is generated such that this program will solve the equations numerically to simulate the behaviour of the system represented by the model.

The information needed to generate the source code in C for the VehicleSim solver is assembled in VehicleSim Lisp as it processes the model description that the user provides.

The symbolic equations generated by VehicleSim Lisp can be viewed and used with other software packages such as Word or Matlab. VehicleSim Lisp is not a complete simulation system as it can generate equations but it does not solve them. Therefore, a C compiler is needed to compile the source code

generated for a VehicleSim solver program and the DLL solvers are built up [27].

The geometric and inertial properties of the rigid bodies that will conform the model are provided as inputs. Forces and torques between the various model's component can be added acting on the corresponding bodies.

The main purpose of each VehicleSim solver is to calculate time histories of the system's variables, this is, the positions, speeds and accelerations of the bodies conforming the system and all user-created variables. These time histories are stored in a binary data file with the extension BIN. The data in a BIN file are organized by variable name and sample number. A companion file, with extension ERD, documents the layout of the BIN file. The ERD header file also contains labelling information for each variable.

Data processing programs for ERD and BIN files obtain the information needed from the ERD file. The high level of automation in the animator and plotter is possible because both are designed to extract the information from ERD files [28].

On the other hand, VehicleSim generates the model's linearised and non-linearised equations of motion in form of differential equations. In addition to this, VehicleSim also provides in form of a Matlab file the linearised state-space model in symbolic form (see Figure 2).

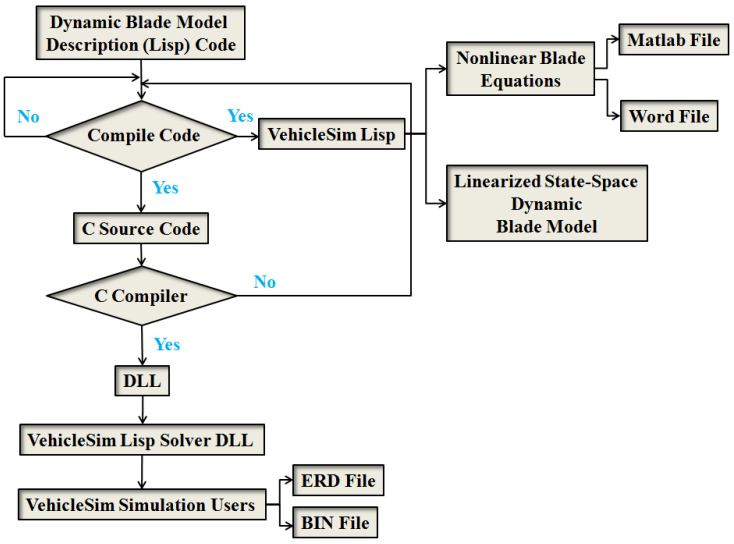

Figure 2: Flow chart of VehicleSim simulation procedure.

3 Spring Pendulum Nonlinear Dynamics

To carry out a comprehensive study of a main rotor blade with two degrees of freedom, a nonlinear mechanical system such as a spring pendulum, is studied and analogies between both system shall be drawn. The pendulum is a system conformed by mass connected to a spring so that the motion that results has characteristics of a simple pendulum as well as a spring. It shows a nonlinear dynamic behaviour with two coupled degrees of freedom in a similar manner as the blade under study. In this section the spring pendulum nonlinear equations for two cases are studied in order to identify the mathematical terms responsible of the energy exchange process and its characteristics.

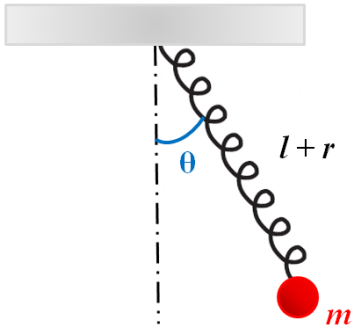

Figure 3: Spring pendulum system.

First, consider a pendulum conformed by a spring with a mass m at its end, dissipation of energy is not considered (see Figure 3). As it can be seen, the spring is arranged to lie in a straight line. l is the spring fixed length, r is the extension from fixed length and $(l + r)$ is the elongated spring length. θ is the angle with the vertical, the motion takes place in the vertical plane. The kinetic energy can be written as:

$$T = \tfrac{1}{2}m\left(\dot{r}^2 + (l+r)^2\,\dot{\theta}^2\right) \tag{2}$$

The potential energy can be expressed as:

$$V(r,\theta) = -mg\,(l+r)\,cos\theta + \tfrac{1}{2}kr^2 \tag{3}$$

Therefore, the Lagrangian is:

$$L = T - V = \tfrac{1}{2}m\left(\dot{r}^2 + (l+r)^2\,\dot{\theta}^2\right) + mg\,(l+r)\,cos\theta - \tfrac{1}{2}kr^2 \tag{4}$$

and the Euler-Lagrange equations are:

$$m\ddot{r} = m\,(l+r)\,\dot{\theta}^2 + mgcos\theta - kr \tag{5}$$

and

$$m\,(l+r)\,\ddot{\theta} + 2m\dot{r}\dot{\theta} = -mgsin\theta \tag{6}$$

In a rotating reference frame, equation (5) is the radial equation completed with the corresponding centrifugal force term $m\left(l+r\right)\dot{\theta}^2$. Equation (6) is the tangential equation which includes the Coriolis force $-2m\dot{r}\dot{\theta}$ [29].

Furthermore, additional information can be obtained considering the system shown in Figure 4, in this case, the amplitude of driving displacement (y_s) and dissipation function are considered. The dissipation will appear in the equations of motion as damping forces.

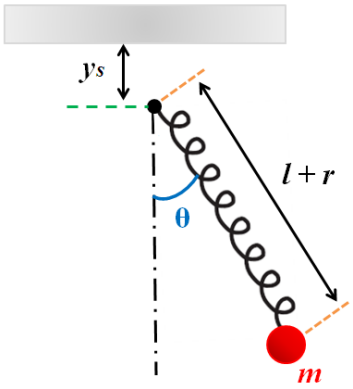

Figure 4: Spring pendulum with displaced attachement point.

Standard processes associated with Lagrange mechanics establish that the equations of motion in this case are:

$$\left(l+r\right)\ddot{\theta}+2\dot{r}\dot{\theta}-\ddot{y}_s sin\theta=-gsin\theta-\left(d_\theta/m\right)\dot{\theta} \tag{7}$$

$$\ddot{r}=-\left(k/m\right)r-\left(d_r/m\right)\dot{r}+\left(g-\ddot{y}_s\right)cos\theta+\left(l+r\right)\dot{\theta}^2 \tag{8}$$

the terms d_r and d_θ are corresponding damping factors of the dissipation forces. These equations can be linearised around the vertical rest position to yield:

$$\delta\ddot{\theta}=-\frac{g}{l+r_0}\delta\theta \tag{9}$$

and

$$\delta\ddot{r}=-\frac{k}{m}\delta r \tag{10}$$

where g is gravity, r_0 is the equilibrium extension and k is the spring stiffness. According to this, the system in Figure 4 has two uncoupled modes of motion with resonant frequencies: $\omega_\theta=\sqrt{g/\left(l+r_0\right)}$ and $\omega_r=\sqrt{k/m}$ for the swing and heave modes, respectively.

In equations (7) and (8), the corresponding modes are coupled by the quadratic terms $2\dot{r}\dot{\theta}$ in the case of (7) and $l\dot{\theta}^2$ in the case of (8). The impact of these terms may be analysed by using the Lindstedt-Poincare method [3]. This is, the solutions of equations (7) and (8) can be expanded as:

$$r\left(t;\epsilon\right)=\epsilon r_1(t)+\epsilon^2 r_2(t)+.. \tag{11}$$

and

$$\theta\left(t;\epsilon\right)=\epsilon\theta_1(t)+\epsilon^2\theta_2(t)+.. \tag{12}$$

where ϵ is a small dimensionless parameter and is of the order of the amplitude of the motion. A change of variable must be introduced $\tau=\omega t$ where ω can be expanded as: $\omega\left(\epsilon\right)=\omega_0+\epsilon\omega_1+\epsilon^2\omega_2+...$

After some algebraic manipulations, r_1 and θ_1 are found to be the solutions to the linearised equations of motion i.e., $r_1\left(\tau\right)=A_r sin\left(\omega_r\tau+\phi_r\right)+r_0$ and $\theta_1\left(\tau\right)=A_\theta sin\left(\omega_\theta\tau+\phi_\theta\right)$; where A_r, A_θ, ϕ_r and ϕ_θ are constants of integration. Further analysis leads to:

$$r_2\left(\tau\right)=\frac{gA_\theta^2}{\omega_r^2}\left(1-\frac{3}{1-4\left(\frac{\omega_\theta}{\omega_r}\right)^2}cos\left(2\omega_\theta\tau+2\phi_\theta\right)\right)+r_0 \tag{13}$$

and

$$\begin{array}{l}\theta_2\left(\tau\right)=-\frac{\omega_\theta\left(\omega_\theta+2\omega_r\right)}{\left(l+r_0\right)\omega_r\left(\omega_r+2\omega_\theta\right)}A_rA_\theta cos\left(\left(\omega_r+\omega_\theta\right)\tau+\phi_1\right)\\ -\frac{\omega_\theta\left(\omega_\theta-2\omega_r\right)}{\left(l+r_0\right)\omega_r\left(\omega_r-2\omega_\theta\right)}A_rA_\theta cos\left(\left(\omega_r-\omega_\theta\right)\tau+\phi_2\right)\end{array} \tag{14}$$

Equations (13) and (14) show that when the swing and heave modes have a 2:1 relationship, the condition $\omega_r=2\omega_\theta$ is satisfied, $r_2\left(\tau\right)$ and $\theta_2\left(\tau\right)$ will tend to infinity, clear indication of the existence of resonance.

A general nth degree of freedom system, has n natural frequencies and n corresponding natural modes. The presence of more than one natural frequency modes may introduce a physical phenomena known as internal resonance, if two or more of these frequencies are commensurable, or nearly commensurable [3].

In the case of the spring pendulum, internal resonance is mathematically represented by the quadratic coupling terms $2\dot{r}\dot{\theta}$ and $l\dot{\theta}^2$, when $\omega_r=2\omega_\theta$. In general, it can be stated that energy exchange in physical systems occurs by virtue of the existence of special relationships between the modal frequencies and the presence of nonlinear coupling terms, which can be of different orders [30].

4 Coupled Flap and Lag Motion Analysis

In most cases for articulated rotors, the flap and lag hinges are mounted simultaneously on the rotor structure. These two degrees of freedom are coupled and the mathematical expression representing the respective motions can become complex and prone to errors if they were to be hand derived. In this section, the nonlinear equations for flap/lag coupled motion are obtained by using VehicleSim, quadratic coupling terms are studied in the equations as well as the ratio 1:2 between flap/lag frequencies, in order to establish the existence of transference of energy between these modes. The reader is reminded that the aerodynamic forces are not considered as this study is focussed only in the coupled dynamics in absence of air flow influence.

4.1 Nonlinear Equations for Flap/Lag Coupled Motion

In order to find analogies between the two systems and to identify these terms on the main rotor blades, the nonlinear equations of motion are obtained using VehicleSim.

Nonlinear flap equation of motion:

$$\ddot{\beta}(I_{blx}cos^2\xi + I_{bly}sin^2\xi + m_{bl}y_{bl}^2cos^2\xi) - m_{bl}y_{bl}sin\xi cos\xi y_{bl}\underbrace{2\dot{\beta}\dot{\xi}}_{(a)} =$$
$$(-cos\xi(-\Omega cos\xi sin\beta(I_{bly}(\dot{\xi}+\Omega\beta) - I_{blz}(\dot{\xi}+\Omega cos\beta)) + \dot{\beta}sin\xi(I_{bly}(\dot{\xi}+\Omega cos\beta)$$
$$-I_{blz}(\dot{\xi}+\Omega cos\beta)) + I_{blx}(\Omega\dot{\xi}cos\xi sin\beta + \dot{\beta}(-\dot{\xi}+\Omega cos\beta)sin\xi) + k_{fj}\beta) + sin\xi$$
$$(\Omega sin\beta sin\xi(I_{blx}(\dot{\xi}+\Omega cos\beta) - I_{blz}(\dot{\xi}+\Omega cos\beta)) + \dot{\beta}cos\xi(I_{blx}(\dot{\xi}+\Omega cos\beta)$$
$$-I_{blz}(\dot{\xi}+\Omega cos\beta)) + I_{bly}(\Omega\dot{\beta}cos\beta cos\xi - \dot{\xi}(\dot{\beta}cos\xi + \Omega sin\beta sin\xi))) + m_{bl}(cos\beta$$
$$(-(\Omega cos\xi)^2(-(-y_{bl}^2)sin\beta) + g(y_{bl}cos\xi)) - cos\xi(y_{bl}(eR\Omega^2 sin\beta))$$
$$-sin\beta(\Omega(\dot{\xi}(2(y_{bl}cos\xi)^2))))) \tag{15}$$

where β is the flap angle, ξ is the lag angle, m_{bl} is the main rotor blade mass, y_{bl} is the blade centre of mass, k_{fj} is the main rotor flap hinge spring stiffness, Ω is the main rotor angular speed, eR is the offset, g is gravity. I_{blx}, I_{bly}, I_{blz} are the blade moments of inertia around their corresponding axis.

Nonlinear lag equation of motion:

$$\ddot{\xi}(I_{blz} + m_{bl}y_{bl}^2) + m_{bl}y_{bl}sin\xi cos\xi\underbrace{y_{bl}\dot{\beta}^2}_{(b)} = cos\xi(I_{blx}\Omega\dot{\beta}cos\xi sin\beta - (I_{bly} - I_{blx})$$
$$sin\xi(\Omega sin\beta)^2) - d_{lj}\dot{\xi} - k_{lj}\xi + \dot{\beta}(\Omega(I_{blz} - I_{bly}cos^2\xi)sin\beta - sin\xi(I_{blx}(\dot{\beta}cos\xi + \Omega$$
$$sin\beta sin\xi) - I_{bly}(\dot{\beta}cos\xi + \Omega sin\beta sin\xi))) + m_{bl}(-sin\xi(gy_{bl}sin\beta) + sin\xi(-eRy_{bl}$$
$$\Omega^2 cos\beta + cos\xi((y_{bl}\Omega sin\beta)^2)) + sin\beta(-\Omega(-y_{bl}(y_{bl}\dot{\beta}) - \dot{\beta}(y_{bl}^2(cos^2\xi - sin^2\xi))))) \tag{16}$$

k_{lj} is the main rotor lag hinge spring stiffness and d_{lj} main rotor lag hinge damping coefficient. The rest of symbols correspond to parameters already described in equation (15).

As it can be seen, two terms have been underlined with (a) and (b) in equations (15) and (16), respectively. These terms are equivalent to those corresponding to the coupling terms described in Section 3 these are $2\dot{r}\dot{\theta}$ and $l\dot{\theta}^2$.

Two considerations must be made: i) VehicleSim provides the nonlinear equations of motion in three dimensions and the spring pendulum equations are two dimensional. Therefore, additional mathematical terms appear in equations (15) and (16) and identical mathematical expressions are not possible, however, this is a first approach in order to understand the complex motion on the blade. ii) The equations contain gravity components in their expressions, being the coupling motion between θ and r degrees of freedom independent of this force.

Taking into account these considerations, analogies can be drawn between the spring pendulum dynamics and main rotor blades.

4.2 Flap/Lag Coupled Dynamics

It should be kept in mind that the blade flap motion is essentially a resonant phenomenon [31, 32]. In order to test the commensurability condition, VehicleSim simulations were carried out with a spring on the flap and lag hinges as well as a damper in the lag hinge. The initial flap angle is $\beta_0 = 0.0175$ rad, and the lag initial angle is $\xi_0 = 0$ rad, these conditions are chosen such that the system has a restoring moment, that has similar dynamical characteristics, as an external force acting on the system because of this test was performed in vacuum. The mass of the blade is 31.06 kg, its length is 4.91 m and the main rotor angular speed is 7.06 Hz/s, various offset values are tested in order to check if the flap/lag modes satisfy the commensurability condition. Once simulations are run, the time history of the flap and lag modes are exported to Matlab analysed using a STFT. The corresponding frequencies are obtained for different offset cases. The results are shown in Table 1.

Offset eR (m)	VehicleSim Flap Frequency (Hz)	VehicleSim Lag Frequency (Hz)
0	7.324	14.648
0.491	7.782	15.548
0.982	8.209	16.403

Table 1: Flap/Lag frequencies with initial conditions $\beta_0 = 0.0175$ rad and $\xi_0 = 0$ rad. Spring in the flap ($k_{fj} = 46772$ Nm/rad) and lag hinges ($k_{lj} = 314938$ Nm/rad). The damping coefficient for the lag hinge damper is $d_{lj} = 349.58$ Nms/rad.

Clearly, for each offset, there is a flap/lag natural frequency ratio 1:2, this is, $\Omega_\xi = 2\Omega_\beta$, which indicates that the commensurability condition is satisfied.

4.3 Energy Exchange

In order to study the existence of energy exchange, this section studies if the dynamics represented in (15) and (16), affected by gravity because of the transference of energy, should be sensitive to any external perturbation. These are solved using a Matlab's standard procedure for ordinary differential equations (ODEs) such as ode45. This approach performs a Runge-Kutta method with a variable time step for efficient calculation. The simulations will be carried out using the following parameters: the blade's mass is 31.06 kg, the hinge offset is 0.491 m, the main rotor angular speed is 0.706 Hz/s and the simulation time is 250 seconds. This configuration should be adequate to find evidence of energy transfer if it exists. The authors show these as an example, other conditions could be chosen and still find similar conclusions.

The proposed study is carried out by analyzing spectrograms obtained when a Short Time Fourier Transform is applied (STFT). In mathematical terms, the

STFT of a signal $X(t)$ can be defined as:

$$S_x(t,\omega) = \int_{-\infty}^{\infty} X(\tau)h(\tau - t)e^{-j\omega\tau}d\tau \tag{17}$$

$X(t)$ is the corresponding signal under study, and $h(t)$ is a finite support window function. The properties of the window function $h(t)$ have a significant effect on the STFT result and should be carefully chosen. The spectrograms of the signals (states' time histories) have been obtained with an overlapping of 99% to get a good compromise between time and frequency resolutions and a 250 seconds time window. The low and high frequency components were neglected. Due to the size of the window, the spectrograms for the first and the last seconds cannot be shown. However, the different frequencies can be clearly recognized.

First, a blade with flap degree of freedom is simulated, where the flap hinge spring is zero. The flap frequencies spectrogram is shown in Figure 5. Two frequencies values are clearly visible. There is a prevalent frequency of flap oscillation at about 0.75 Hz and an additional frequency is presented, being this a harmonic.

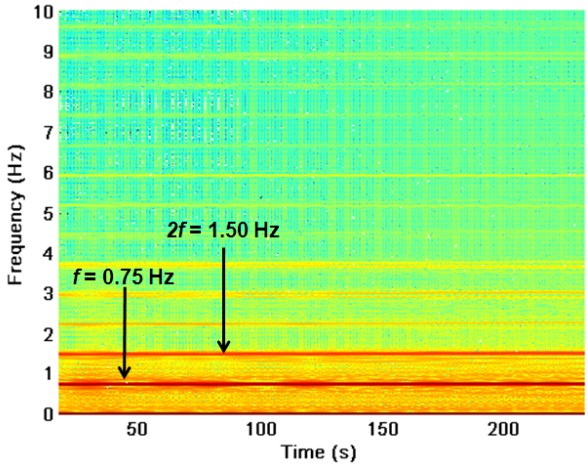

Figure 5: Flap mode frequencies spectrogram when there is no coupled flap/lag, $m_{bl} = 31.06$ kg, $k_{fj} = 0$, eR $= 0.491$ and $\Omega = 0.706$ Hz/s.

Secondly, another simulation for a blade with only lag degree of freedom is carried out, there is a lag damper fitted in the lag hinge ($d_{lj} = 4.4958$ Nms/rad), the lag hinge spring coefficient is $k_{lj} = 314938$ Nm/rad and the initial lag angle is $\xi_0 = 0.0175$ rad [8]. The damper magnitude is decreased in order to ease the exchange energy between the flap and lag degrees of freedom. Figure 6 shows the lag frequency spectrogram obtained in this case, clearly there is a prevalent amplitude of lag oscillation at about 5 Hz.

Third, a blade with flap and lag degrees of freedom is also simulated, in this case, the lag hinge damper is $d_{lj} = 4.4958$ Nms/rad and the initial lag angle

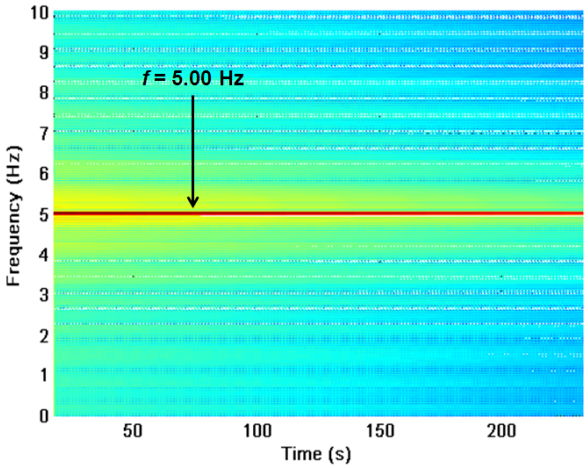

Figure 6: Lag mode frequencies spectrogram when there is no coupled flap/lag, $m_{bl} = 31.06$ kg, $d_{lj} = 4.4958$ Nms/rad, $k_{lj} = 314938$ Nm/rad, eR $= 0.491$ and $\Omega = 0.706$ Hz/s.

is $\xi_0 = 0$ rad. In this case, the flap and lag degrees of freedom are coupled and the corresponding parameters for each of them remain constant. However, each degree of freedom must be separately studied in order to test the energy exchange between them. As a consequence of this, the two degrees of freedom are plotted in separate graphs. The flap spectrogram is shown in Figure 7, as it can be seen, a main frequency of 0.82 Hz is presented and harmonics are clearly seen. In addition to this, the lag spectrogram is shown in Figure 8, a main frequency of 0.82 Hz is seen as well as their corresponding harmonics.

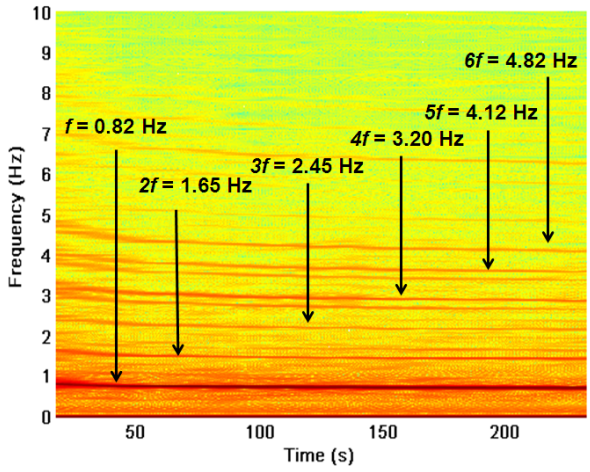

Figure 7: Flap mode frequencies spectrogram when there is coupled flap/lag, $m_{bl} = 31.06$ kg, $k_{fj} = 0$, $d_{lj} = 4.4958$ Nms/rad, $k_{lj} = 314938$ Nm/rad, eR $= 0.491$ and $\Omega = 0.706$ Hz/s.

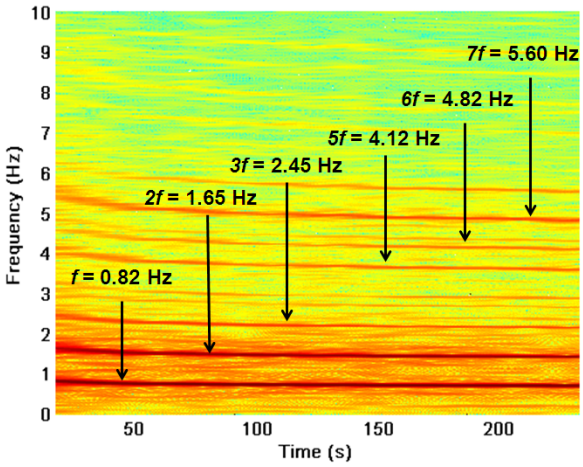

Figure 8: Lag mode frequencies spectrogram when there is coupled flap/lag, $m_{bl} = 31.06$ kg, $k_{fj} = 0$, $d_{lj} = 4.4958$ Nms/rad, $k_{lj} = 314938$ Nm/rad, eR = 0.491 and $\Omega = 0.706$ Hz/s.

The spectrograms obtained (figures 7 and 8) have clearly shown the exchange of energy between the flap/lag degrees of freedom. The main frequencies become equal and harmonics of these frequencies are also presented in both spectrogram. However, when both degrees of freedom are uncoupled (figures 5 and 6), the corresponding spectrograms showed different shape, being their frequencies clearly different. These results agree with the expected behaviour.

4.4 Poincare' Maps

Nonlinear systems often exhibit periodic or quasi-periodic motions, among other characteristic behaviours. Stability analysis in nonlinear systems often requires different approaches/methods to those in linear cases. In this article, the Poincare' map method is used in order to shed some light on the stability properties of the coupled flap/lag system.

The flap amplitude Poincare' map is shown in Figure 9 as well as the flap displacement. As it can be seen, the system displays stable behaviour. In this case, the flap hinge was uncoupled and no lag hinge was included in the simulation.

Similarly, a Poincare' map and the lag displacement are plotted for the case of a lag hinge (in absence of flap degree of freedom). In this case, the lag damper is fitted in the lag hinge, as a consequence of this, the lag amplitude is decreasing, see Figure 10. It is also seen how the lag amplitude versus lag angular velocity shows a stable behaviour.

Now, the case when both modes are on the blade will be studied. The differential equations of motion are coupled, whereby changes in the flap angle affect

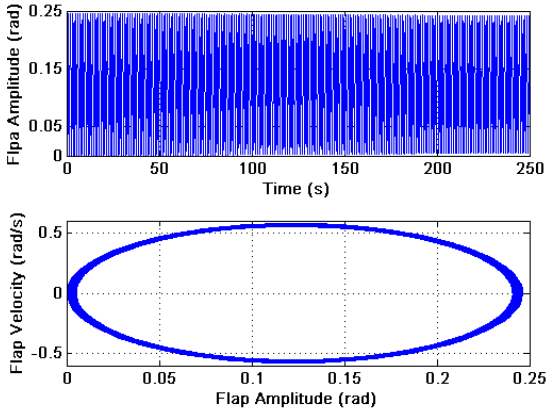

Figure 9: Time response and Poincare' map of an uncoupled blade flap hinge system.

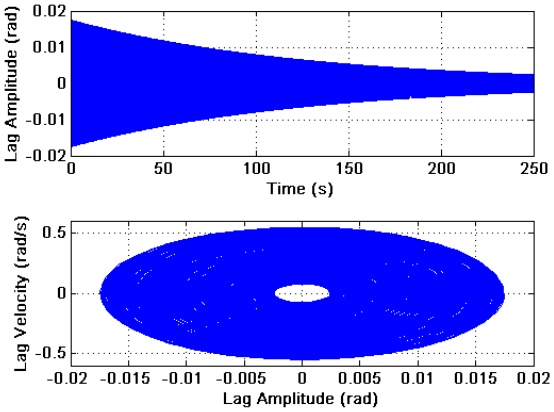

Figure 10: Time response and Poincare' map of an uncoupled blade with lag hinge but no flap.

the equation governing lag motion, and vice versa. Physically, this leads to an interaction between the flap and lag modes of vibration, as it has been shown in figures 7 and 8. This behaviour can also be analysed in the corresponding Poincare' maps. Figure 11 shows the stability of the flap mode when the lag is coupled, the flap amplitude displays a slight drop. This is lower than in the case of uncoupling, see Figure 9. As it can be seen, the lag mode shows its impact on the flap mode for the coupled modes, and this impact diminishes the flap amplitude damping. Although, figures 9 and 11 do not display large different in their flap amplitudes, however, they are suitable to reach the proposed objectives by the authors.

The Poincare' map is obtained for the case of the lag when both flap/lag are coupled, is shown in Figure 12. In this case, the lag degree of freedom is

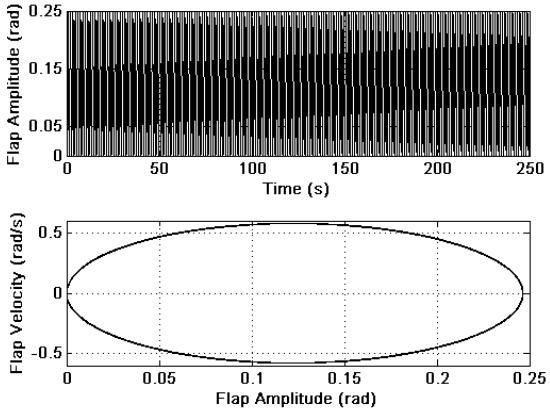

Figure 11: Time response and Poincare' map of a coupled blade flap hinge system.

also influenced by the flap dynamics. There is a harmonic behaviour, which indicates the effect of a forced response [33–35]. Figures 11 and 12 present a relevant practical significance due to robust control theory will be applied to this system. The Poincare' maps can be used as a design tool in order to derive the parameters of the controller in terms of the desired frequency and amplitude. In addition, explicit expressions can be obtained with the help of these maps [36, 37]. On the other hand, the flap and lag oscillations presented in rotor blades can be become unstable and the control law should be applied to the Poincare' map which governs samples of the system. Being this approach suitable to systems such as helicopters [38].

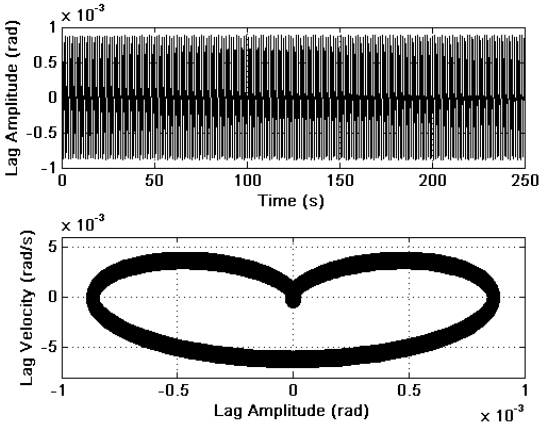

Figure 12: Time response and Poincare' map of a coupled blade with lag hinge system.

5 Conclusions

This paper identifies and studies mathematical terms that represent the exchange of energy on a rotorcraft main rotor blade with flap and lag degrees of freedom, the model implemented reproduces the nonlinear dynamical behaviour. This has been modelled in VehicleSim, a program that allows to define the systems as a composition of several bodies and ligatures by using a parent/child structure. Implementation issues, related to the use of VehicleSim multibody software, have also been discussed and their advantages have been contrasted with respect to existing work. The mathematical expressions representing the flap and lag motions can become quite complex and are prone to errors if they were to be hand derived. VehicleSim provides the nonlinear equations of a system in three dimensions in an automated manner.

Helicopter modelling is a challenging task due to its inherent nonlinearities. Helicopter rotor dynamics are highly nonlinear, and resonance effects and energy exchanges are not straigth-forward to identify. For this purpose, and equivalent nonlinear system (spring-pendulum) has been revised, commensurability and resonance conditions were identified in some of the nonlinear terms of its dynamical equations. By studying closely the nonlinear equations of the rotor blade, parallel conclusions were drawn for the flap/lag system, the commensurability condition that could be expected from the corresponding coupled terms in the equations were shown to exist by analyzing simulation data obtained using VehicleSim. In fact, a relation 1:2 between the flap/lag oscillation modes was clearly satisfied.

The transference of energy between the flap and lag modes was analysed by spectral methods. In addition to this, Poincare' maps have been obtained, allowing to analyse the system stability response. The results have shown the impact between the flap and lag modes as well as a manifest transference of energy between them. This was carried out for a low rotor angular speed, gravity action and a low lag damper fitted in the lag hinge.

The aerodynamics actions have not been considered due to the spring-pendulum equations have been provided without any aerodynamic loads, so any comparison between the two systems must be carried out under similar conditions. Furthermore, this work is focused on the blade dynamical analysis in order to study this mechanism in detail and to extend the results to more complex environments such as the aerodynamic loads. Being this the main goal for future researches.

References

[1] Newman, S. The Foundations of Helicopter Flight. Edward Arnold (1994).

[2] Chen, R.T.N. Flap-Lag Equations of Motion of Rigid, Articulated Rotor Blades with Three Hinge Sequences. NASA Technical Memorandum 100023 (1987).

[3] Nayfed, A.H., Mook, D.T. Nonlinear Oscillations. NY: Wiley-Interscience (1979).

[4] Saved, M., Kamel, M. Stability Study and Control of Helicopter Blade Flapping Vibrations. Applied Mathematical Modelling. 35, 2820-2837 (2011).

[5] Saved, M., Kamel, M. 1:2 and 1:3 Internal Resonance Active Absorber for Non-Linear Vibrating System. Applied Mathematical Modelling. 36, 310-332 (2012).

[6] Santos, I.F., Saracho, C.M., Smith, J.T., Eiland, J. Contribution to Experimental Validation of Linear and Non-linear Dynamic Models for Representing Rotor-Blade Parametric Coupled Vibrations. Journal of Sound and Vibration. 271, 883-904 (2004).

[7] Tekin, A., Ozkaya, E., Bagdath, S.M. Three-to-one Internal Resonance in Multiple Stepped Beam Systems. Applied Mathematics and Mechanics (English Edition). 30(9), 1131-1142 (2009).

[8] Yan, S., Dowell, E.H., Lin, B. Effects of Nonlinear Damping Suspension on Nonperiodic Motions of a Flexible Rotor in Journal Bearings. Nonlinear Dyn. 78, 1435-1450 (2014).

[9] Nayfeh, A.H., Mook, D.T., Larry, R., Marshall, L.R. Nonlinear Coupling of Pitch and Roll Modes in Ship Motions. Journal of Hydronautics. 7(4), 145-152 (1973).

[10] Ibrahim, R.A., Grace, I.M. Modeling of Ship Roll Dynamics and Its Coupling with Heave and Pitch. Mathematical Problems in Engineering. (2009). doi:10.1155/2010/934714.

[11] Evangelou, S.A., Limebeer, D.J.N., Tomas Rodriguez, M. Suppression of Burst Oscillations in Racing Motorcycles. ASME J. Applied Mechanics. 80(1), 011003 (2012).

[12] Hamed, Y.S., EL-Sayed, A.T, El-Zahar, E.R. On Controlling the Vibrations and Energy Transfer in MEMS Gyroscope System with Simultaneous Resonance. Nonlinear Dyn. 83, 1687-1704 (2016).

[13] Chun-Ni, W., Ya, W., Jun, M. Calculation of Hamilton Energy Function of Dynamical System by using Helmholtz Theorem. Acta Physica Sinica. 65, 24 (2016).

[14] Xin-Lin, S., Wu-Yin, J., Jun, M. Energy Dependence on the Electric Activities of a Neuron. Chinese Physics B. 24, 12 (2015).

[15] Li, F., Yao, C. The Infinite-Scroll Attractor and Energy Transition in Chaotic Circuit. Nonlinear Dyn. 84, 2305 (2016).

[16] Sarasola, C., Torrealdea, F.J., d'Anjou, A., Moujahid, A., Grana, M. Energy Balance in Feedback Synchronization of Chaotic Systems. Physical Review E. 69, 011606 (2004).

[17] Hou, Y., Fang, P., Nan, Y., Du, M. Synchronization Investigation of Vibration System of Two Co-Rotating Rotor with Energy Balance Method. Advances in Mechanical Engineering. 8(1), 1-19 (2016).

[18] Zhou, S., Cao, J., Inman, D., Lin, J., Li, D. Harmonic Analysis of Nonlinear Tristable Energy Harvesters for Performance Enhancement. Journal of Sound and Vibration. (2016). http://dx.doi.org/10.1016/j.jsv.2016.03.017.

[19] Bauchau, O.A., Bottasso, C.L., Nikishkov, Y.G. Modeling Rotorcraft Dynamics with Finite Element Multibody Procedures. Mathematical and Computer Modelling. 33(10-11), 1113-37 (2001).

[20] Stupar, S., Simonovic, A., Jovanovic, M. Measurement and Analysis of Vibrations on the Helicopter Structure in Order to Detect Defects of Operating Elements. Scientific Technical Review. 62(1), 58-63 (2012).

[21] Leishman, J.G. Principles of Helicopter Aerodynamics. Cambridge University Press (2007).

[22] Ilkko, J., Hoffren, J., Siikonen, T. Simulation of a Helicopter Rotor Flow. Journal of Structural Mechanics. 44(3), 186-205 (2011).

[23] Magari, P.J., Shultz, A., Murthy, V.R. Dynamics of Helicopter Rotor Blades. Computers & Structures. 29(5), 763-776 (1988).

[24] Johnson, W. Helicopter Theory. Princeton, NJ: Princeton Univ. Press (1980).

[25] Castillo-Rivera, S. Advanced Modelling of Helicopter Nonlinear Dynamics and Aerodynamics. PhD Thesis. School of Engineering and Mathematical Sciences. City University London. United Kingdom. (2015). URL: http://openaccess.city.ac.uk/13169/.

[26] Marichal, G.N., Tomas-Rodriguez, M., Hernandez, A., Castillo-Rivera, S., Campoy, P. Vibration Reduction for Vision System on Board UAV Using a Neuro-Fuzzy Controller. Journal of Vibration and Control. 20(15), 2243-2253 (2013).

[27] Mechanical Simulation Corporation. VehicleSim Solver Programs Reference Manual. Mechanical Simulation. http://www.carsim.com (1996-2008). Accessed 22 January 2017.

[28] Mechanical Simulation Corporation. VehicleSim Browser Reference Manual for BikeSim, CarSim, and TruckSim. Mechanical Simulation. http://www.carsim.com (1996-2008). Accessed 22 January 2017.

[29] Morin, D. Introduction to Classical Mechanics. Cambridge University Press (2007).

[30] Shaeri, A., Limebeer, D.J.N., Sharp, R.S. Nonlinear Steering Oscillations of Motorcycles. 43^{rd} IEEE Conference on Decision and Control. December 14-17, Atlantis, Paradise Island, Bahamas (2004).

[31] Yun, C.H., Kim, D.S., Kim, S.J. Stability Augmentation of Helicopter Rotor Blades using Passive Damping of Shape Memory Alloys. KSAS International Journal. 7(1), 137-147 (2006).

[32] Bramwell, A.R.S., Done, G., Balmford, D. Bramwell's Helicopter Dynamics. Butterworth-Heinemann (2001).

[33] Gilliam, T.D. Numerical Modeling of the Dynamic Response of a Multi-Bilinear-Spring Support System. University of Kentucky. Master's Thesis. Paper 137 (2010).

[34] Jankowski, K. Dynamics of Double Pendulum with Parametric Vertical Excitation. Technical University of Lodz. Master of Science Thesis (2011).

[35] de Paula, A.S., Savi, M.A., Lagoudas, D.C. Nonlinear Dynamics of a SMA Large-Scale Space Structure. J. of the Braz. Soc. of Mech. Sci. & Eng. Special Issue. Vol. XXXIV, 401-412 (2012).

[36] Aguilar L.T, Boiko, I.M., Fridman, L.M., Freidovich, L.B. Generating Oscillations in Inertia Wheel Pendulum via Two-Relay Controller. International Journal of Robust and Nonlinear Control. 22(3), 318-330 (2011).

[37] Aguilar L.T, Boiko, I.M., Fridman, L.M., Iriarte, R. Poincare Map-Based Design. Self-Oscillations in Dynamic Systems. 63, 493-502. Springer International Publishing. (2015).

[38] Schmitt, J.M., Bayly, P.V., Peters, D.A. Stabilization of Periodic Flap-Lag Dynamics in Rotorcraft. IUTAM Symposium on New Applications of Nonlinear and Chaotic Dynamics in Mechanics. 63, 39-52. Springer Netherlands. (1999).